The prediction of carbonyl groups during photo-thermal and thermal aging of polymers using artificial neural networks

H. Maouz[1,*], L. Khaouane[1], S. Hanini[1], Y. Ammi[1,2], M. Laidi[1], H. Benimam[1]

[1]Laboratory of Biomaterials and Transport Phenomena (LBMPT), University of Médéa, Quartier Aïn d'Heb, 26000. Algeria
[2]University center- Faculty of Science and Technology- Department of Process Engineering- Relizane Algeria

* Corresponding authors: maouz.hadjira@yahoo.com

ARTICLE INFO

ABSTRACT/RESUME

Abstract: *Major advances in modeling and control are required to meet future technical challenges in polymers manufacturing. This work investigates the recent applications of artificial neural network (ANN) in modeling the carbonyl groups during photo-thermal and thermal aging of PE, LDPE, PP, PVC, PS and EPDM. A set of 2450 data points for carbonyl index (CI) contains 15 polymer systems which are 5 pure, 5 binary, 3 tertiary and 2 quaternary systems, and 577 data points for concentration of carbonyl ([CO])including 4 systems, within 1 pure, 1 binary, 1 tertiary and 1 quaternary system, were used to test the neural networks proficiency. For the most promising neural network models, the predicted carbonyl index and concentration of carbonyl values of the total dataset were compared to measured carbonyl index and concentration of carbonyl values; good correlations were found (R= 0.9471 for ANN1 and R= 0.9830 for ANN2). The root mean square errors for the total dataset were 0.0958 and 0.0291 mol/l for CI and [CO] respectively. The comparison between the first and the second model proves the importance of the common properties of polymers and their additives in order to distinguish them.*

I. Introduction

The polymers can be of natural and synthetic origin, presented in very various forms liquid to the solid used as a material of the structure. Among various polymers, polyethylene (PE), low-density polyethylene (LDPE), polypropylene (PP), poly(vinyl chloride) (PVC), polystyrene (PS) and ethylene propylene diene monomer (EPDM) are synthetic plastic and rubber produced at an industrial scale. There is a growing market for the production of polymers due to their low cost and increased use; and the very wide range of applications of the polymeric materials explains why their study quickly became a very important subject.

Polymer materials possess some advantages, for instance, light-weight, high strength, anti-rust, and easily processable characters that differentiate them from inorganic materials and metals [1]. Whereas, among of the disadvantages of the use of polymers is that they degrade when they are subjected to the aggression of environmental factors, such as abrasion, heat, light, radiation and the action/impact of chemicals or micro-organisms. These factors cause the aging of polymeric materials.

Aging, as explained in the literature [2–6], is a process that occurs in polymeric materials during a

specified period of time, and that usually results in changes in physical and/or chemical structure and consequently alters the properties of the polymeric material. Colin and coworkers [7] defined aging as a slow and irreversible variation as a function of time (in use conditions) of a material structure, morphology or composition leading to a detrimental change in its use properties. There are a wide variety of polymer aging types. The different types of aging, defined according to the main environmental aging stress, can be classified into two main categories: physical or chemical. The aging of polymeric materials (under the action of heat, UV radiation and oxygen) follows radical processes which lead to the formation of oxidized chemical functions such as alcohols, ketones, carboxylic acids and reduces molecular mass, resulting in the deterioration of mechanical properties and the creation of unnecessary materials under unpredictable weather conditions [6,8]. Carbonyl groups have been used to evaluate/measure the amount of polymers degradation during ultraviolet radiation and heat in the presence of oxygen over the time. Growth of carbonyl groups indicates extent of polymer degradation. Polymers are commonly protected against such deterioration by the addition of antioxidants, light and heat stabilizers [9]. Almost all synthetic plastics require stabilization against adverse environmental effects. It is necessary to find means to reduce or prevent damage induced by environmental components such as heat, light or oxygen [10].

Aging is a complex problem to study in practice because it usually proceeds slowly in smooth service conditions of materials, and lifetime reaches typically several dozens of years. It is therefore not advisable to test and qualify polymeric materials for a given application on a natural aging foundation [7]. The very particular field of aging of polymer materials does not escape the attempts of modeling, and industrial demand is strong for the development of numerical calculation tools allowing to criticize and enhance the representativeness of accelerated aging testing methodologies and to predict the lifetime of polymer materials [11].

Many researchers have adopted artificial intelligence approaches to predict material behaviors, characteristics and attributes under changing circumstances [12]. These approaches, such as Artificial Neural Networks (ANN), has received much attention as a computational approach providing an alternative and complementary way for modeling, due to its ability to cope with complex and ill-defined problems in many scientific fields, for example: in the modeling of solar radiation variables [13], modeling of an industrial process of pleuromutilin fermentation [14], prediction of acute herbicide toxicity [15], and prediction of the rejection of organic compounds [16], etc., where the ANN models knew a very promising development which improved the performance of the existing statistical approaches [17].

An ANN does not require the explicit expression of the physical meaning of the system or process under study and is considered as belonging to the group of "black box" models. These models make possible the study of the relationship between the input and output variables of the process with only a limited number of experimental runs [18, 19]. ANN techniques open new possibilities in classifying and generalizing available experimental results [20]. The ANN approach was recently introduced into the field of wear of polymers and it was shown that ANN is a helpful mathematical tool in the structure–property analysis of polymers based on a limited number of measurement results [21–25].

To the best of our knowledge, no studies have been reported in the literature that has used ANN for modeling the carbonyl groups during photo-thermal and thermal aging of the polymers (PP, LDPE, PVC, PS, PE and EPDM) in the presence of additives (antioxidants, stabilizers and pigments…). The objective of the present study is to develop methodologies based on neural networks for the modeling of the photo-thermal and thermal aging process and this for the purpose of prediction of parameters' evolutions, which are difficult to measure online (carbonyl index and concentration of carbonyl), using easily measurable variables. For this, two neural models of feed-forward type were constructed.

II. Methodology and modeling

The procedure of modeling of carbonyl groups in polymers under the action of radiation and/or temperature (photo-thermal and thermal aging) includes four essential steps: collection of experimental data as complete as possible, pretreatment and analysis of the data, choice of the parameters of the neural network and saving ANN parameters.

II.1. Artificial neural networks

Artificial neural networks (ANNs) are information processing systems that have specific performance characteristics that are similar to biological neural networks [20]. To suggest an ANN model, experimental results should be available [25]. The great advantages of these models is their ability to learn (store experimental knowledge), generalize (make the knowledge available) or extract automatically rules from complex data [26]. One of the most popular neural network paradigms applied to the modeling of a wide range of nonlinear systems, is the feed-forward back propagation neural network (FFNN) [27], which has been used throughout this paper with forecasting horizon and supervised learning.

The fundamental unit or building block of the ANN arranged in layers and are interconnected by weights and biases between the layers. The input layer receives inputs (x_i) from the real world and each succeeding layer receives weighted outputs (w_{ji}, x_i) from the preceding layer as its input resulting therefore a feed-forward ANN, in which is called an artificial neuron [22]. The neurons are each input is feed-forward to its succeeding layer where it is treated. The outputs of the last layer constitute the outputs (y_j) to the real world. A schematic representation of a feed-forward MLP neural network is shown in Figure 1.
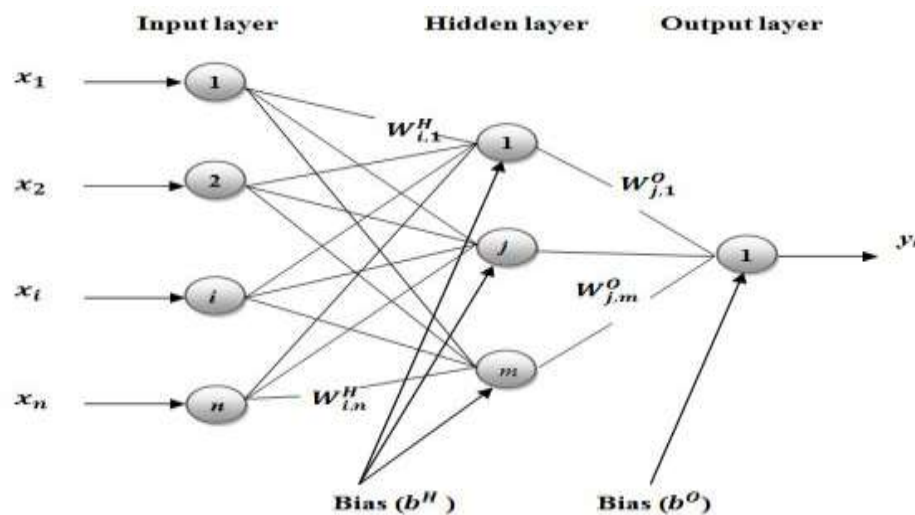
Figure 1. *Three layers feed-forward neural network*

The output is computed by means of a transfer function, also called activation function. It is desirable that the activation function has a sort of step behavior. Furthermore, because continuity and derivability at all points are required features of the current optimization algorithms, typical activation functions which fulfill these requirements are [28]: Hyperbolic tangent sigmoid (tansig): $(a) = \frac{e^a - e^{-a}}{e^a + e^{-a}}$, logarithmic sigmoid (logsig): $f(a) = \frac{1}{1 + e^{-a}}$, pure linear (purelin): $f(a) = a$, exponential (exponential): $f(a) = e^{-a}$ and sin transfer function (sine): $f(a) = \sin(a)$.

II.2. Data collection, division, pretreatment and analysis

The experimental data used for this work has been reported by [29–41]. The total database collected from the literature was divided into two parts based on the effect of radiation and/or temperature on the various polymer systems.
(1) The first data set "D1" is used to predict the evolution of carbonyl index (CI) during photo-thermal aging of the systems polymers (PP, LDPE, PVC, PS and PE). The inputs considered for this database are: aging time (h), aging conditions (The power of the radiation source (kw) and temperature (°C)), the percentage concentrations of polymers and additives (X_1 (% w/w), X_2 (% w/w), X_3 (% w/w), X_4 (% w/w)), pseudo density of the polymers (g/cm^3) and thickens film (µm).
(2) The second data set "D2" is used to follow the evolution of concentration of carbonyl [CO] during thermal aging of the systems polymers (PE and EPDM). The inputs chosen for this database are: aging time (h), temperature (°C), the percentage concentrations of polymers and additives (X_1 (% w/w), X_2 (% w/w), X_3 (% w/w), X_4 (% w/w)) and pseudo molecular weights (kg/mol) of polymers and additives.

The choice of the input and output variables was based on the effect of aging conditions (radiation and/or temperature) on the carbonyl groups as a function of aging time, the need to describe the different polymer systems (polymers and polymers with additives) and the necessity to differentiate between the carbonyl groups data of several polymeric systems. Carbonyl groups have been used to evaluate/measure the amount of polymers

H. Maouz et al

degradation during ultraviolet radiation and heat in the presence of oxygen over the time. Growth of carbonyl groups indicates extent of polymer degradation [42, 43].

The pseudo density of the polymers (g/cm^3) was calculated as follows:

$$\rho_p = \sum_{i=1}^{n} \rho_i x_i \qquad (1)$$

where ρ_i is the density of the pure polymers (g/cm^3) which are presented in Table1 and x_i represents the percentage concentration of polymers and additives. It can be seen that the percentage concentrations of additives are small and do not exceed 2%, and the density of these additives is negligible, for that we seize the density of the polymers is taken as a differentiation parameter between the different polymer systems.

Therefore: $\rho_p = \rho_1 x_1 \qquad (2)$

$$\rho_1 98\% < \rho_p < \rho_1 100\%$$

The Pseudo molecular weight (Kg/mol) is defined by the following relationship:

$$M_{wp} = \sum_{i=1}^{n} M_{wi} x_i \qquad (3)$$

Where M_{wi} is the molecular weights of the polymers and additives (Kg/mol), given in Table 1. Whereas n=1 for pure systems, n=2 for binary systems, n=3 for ternary systems and n=4 for quaternary systems. The pseudo molecular weight is used to distinguish between polymers and additives (EPDM, PE, Irganox 1010, Chimassorb 944 and Peroxyde de dicumyle).

Table 1. Density of polymers and molecular weight used for calculating pseudo density and pseudo molecular weight of polymer systems

	D1		D2		
Polymers	Density ρ(g/cm^3)	Reference	Polymer and additive	Molecular weights M$_W$ (Kg/mol)	Reference
PE	0.932	[44]	**EPDM**	150	[40]
LDPE	0.92	[45]	**PE**	220	[41]
PVC	1.4	[41]	**Irganox 1010**	1.178	
PP	0.905	[46]	**Chimassorb 944**	2-3.1	[40]
PS	1.06	[47]	**Dicumyl peroxide**	0.27037	

Figure S1 (see supplementary data) display the numbers of polymer systems used in the data sets (D1 and D2) and explain the method of calculation of the percentages concentration of different polymers and additives.

X₁: is the percentage concentration of pure polymers (PVC, PS, PP, LDPE, PE and EPDM); **X₂, X₃, X₄**: percentage concentrations of additives, irrespective of the type of additives.

The source and range of the inputs and outputs variables for each polymer system are summarized in Tables S1 and S2 (see supplementary data).

II.3. Model development

The whole first database was randomly split into three subsets: 1716 data points (70%) for the training phase, 367 points (15%) for the validation phase and 367 data points (15%) for the testing

phase of the model (ANN1). Similarly, the second data set is randomly divided into three subgroups: 347 data points (60%) for the training phase, 115 points (20%) for the validation step and 115 data points (20%) for the testing phase of the model (ANN2). The validation set is used in parallel with the training set.

The tow ANNs contain three layers of neurons: the input layer has nine neurons for ANN1 and seven neurons for ANN2, a one hidden layer with a number of active neurons optimized during training, and one output layer with one unit that generated the value of CI for ANN1 and [CO] for ANN2. The number of neurons in the hidden layer varies depending on the performance of the network during the training phase. Primarily, the number of hidden neurons was selected within a range of 3 to 35 neurons. The tansig, the logsig, the exponential, the purelin and the sine transfer functions were used in the hidden layer and the output layer. The training algorithm used in this work is the quasi-Newton BFGS (Broyden–Fletcher–Goldfarb–Shanno) algorithm. For each

ANN, the optimal hidden neurons and transfer function were selected by trial and error process. The ANNs modeling of the carbonyl groups during photo-thermal and thermal aging of the polymers (PE, LDPE, PP, PVC, PS and EPDM) was performed using STATISTICA software.

III. Results and discussion

III.1. Models performances

In the present study, two neural network models were developed with the aim of predicting the CI and [CO]. Table 2 shows the structure of the optimized ANN models.

Table 2. Structures of the optimized ANN models

ANN models	Training algorithm	Input layer	Hidden layer		Output layer	
		Neurons Number	Neurons number	Activation function	Neurons number	Activation function
ANN1	BFGS quasi-Newton	09	21	Tansig	01	Sine
ANN2	(*trainbfg*)	07	11	Exponential	01	Logsig

The plot and the parameters of the linear regression were, straight forwardly, obtained using, **"Postreg"** MATLAB function. Figures 2 show the total agreement plots for the carbonyl index and concentration of carbonyl with agreement vectors approaching the ideal, ($[\alpha, \beta, R]$ = [0.9994, 9.9025e-4, 0.9471] for the total database) for CI; ($[\alpha, \beta, R]$ = [0.9700, 0.0058, 0.9830] for the total database) for [CO].

(a)	(b)
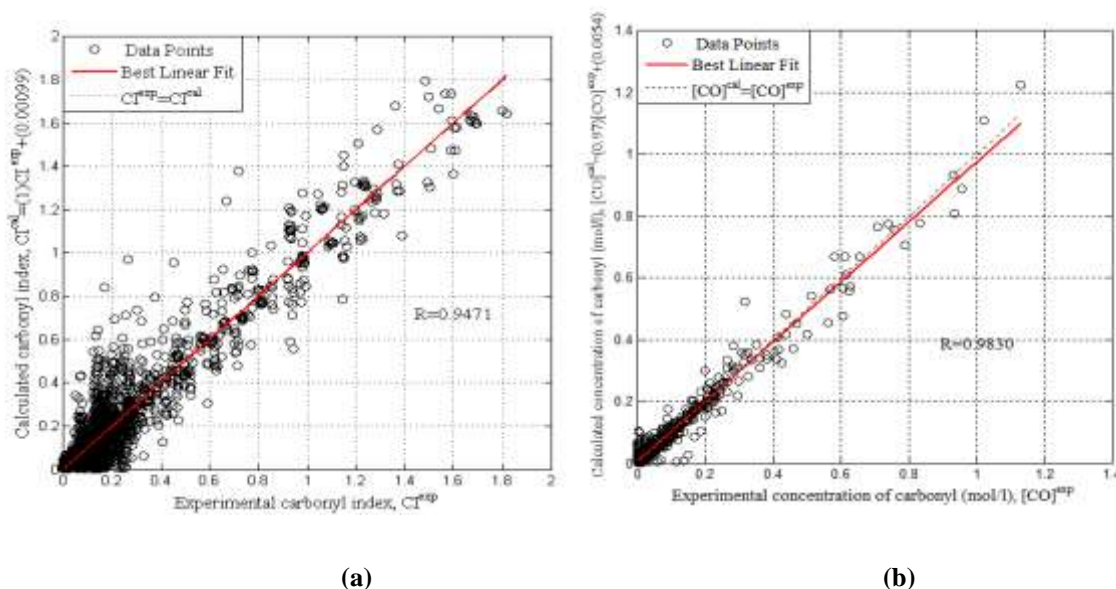
Figure 2. *Regression analysis plot for the optimum model between experimental and calculated (**a**): carbonyl index and (**b**): concentration of carbonyl.*

Table 3 shows the vectors of linear regression for the neural models (ANN1 and ANN2). Clearly, the proposed neuronal approach gives satisfactory results with regression vector values approaching the ideal [α =1 (slope), β =0 (y intercept), R=1 (correlation coefficient)] in the adjustment of the profiles of ANN1 and ANN2. The performance of each model was evaluated in terms of correlation

coefficient (*R*) and root mean square error (*RMSE*). This last was used to determine the modeling error between the models' calculated and experimental values of responses. *RMSE* is defined as follows [48–50]:

$$RMSE = \sqrt{\sum_{i=1}^{n} \frac{(Y_{i,exp} - Y_{i,cal})^2}{n}} \tag{4}$$

where n is the total number of data points; $Y_{i,\,exp}$ is the experimental value and $Y_{i,\,cal}$ represents the calculated value from the neural network models.

Table 3. *Linear regression vectors [Linear Equation: $Y_{i,cal} = \alpha Y_{i,exp} + \beta$]*

		α	β	R	RMSE
ANN1	**Training phase**	1.0012	3.9710e-07	0.9512	0.0951
	Validation phase	0.9705	0.0094	0.9326	0.1098
	Test phase	1.0212	-0.0029	0.9427	0.1058
	Total	0.9994	9.9025e-4	0.9471	0.0958
ANN2	**Training phase**	0.9977	0.0046	0.9854	0.0022
	Validation phase	0.9886	0.0055	0.9887	0.0018
	Test phase	0.9901	0.0050	0.9722	0.0309
	Total	0.9700	0.0054	0.9830	0.0291

The weights and bias of the optimized ANN models are listed in Table S3 and S4 (see supplementary data) where W^I is the input and hidden layer connection weight matrix, W^H is the hidden and output layer connection weight matrix, b^H is the hidden neurons bias and b^O is the output neuron bias. From the optimized ANN1 and ANN2, we can express carbonyl index and concentration of carbonyl by a mathematical models that incorporates all inputs x_i (time, the power of the radiation source, temperature, X_1, X_2, X_3, X_4, thickness film and pseudo density) for ANN1 and (time, temperature, X_1, X_2, X_3, X_4 and pseudo molecular weight) for ANN2 within it as follows:

The instance outputs Z_j of the hidden layer (ANN1)

$$Z_j = f_H\left[\sum_{i=1}^{9} w_{ji}^I x_i + b_j^H\right] = \frac{exp\left(\sum_{i=1}^{9} w_{ji}^I x_i + b_j^H\right) - exp\left(-\sum_{i=1}^{9} w_{ji}^I x_i + b_j^H\right)}{exp\left(\sum_{i=1}^{9} w_{ji}^I x_i + b_j^H\right) + exp\left(-\sum_{i=1}^{9} w_{ji}^I x_i + b_j^H\right)} \tag{5}$$

j=1, 2, 3,…21. The output CI:

$$CI = f_O\left[\sum_{j=1}^{21} w_{1j}^H Z_j + b_k^O\right] = sin\left(\sum_{j=1}^{21} w_{1j}^H Z_i + b_k^O\right) \tag{6}$$

The combination of equations 5 and 6 leads to the mathematical formula for carbonyl index taking into account all the inputs x_i:

$$CI = sin\left(\sum_{j=1}^{21} w_{1j}^H \left[\frac{exp\left(\sum_{i=1}^{9} w_{ji}^I x_i + b_j^H\right) - exp\left(-\sum_{i=1}^{9} w_{ji}^I x_i + b_j^H\right)}{exp\left(\sum_{i=1}^{9} w_{ji}^I x_i + b_j^H\right) + exp\left(-\sum_{i=1}^{9} w_{ji}^I x_i + b_j^H\right)}\right] + b_1^O\right) \tag{7}$$

The instance outputs Z_j of the hidden layer (ANN2):

$$Z_j = f_H\left[\sum_{i=1}^{7} w_{ji}^I x_i + b_j^H\right] = exp\left(-\sum_{i=1}^{7} w_{ji}^I x_i + b_j^H\right) \tag{8}$$

j=1, 2, 3,… 21. The output [CO]:

$$[CO] = f_O\left[\sum_{j=1}^{11} w_{1j}^H Z_j + b_k^O\right] = \frac{1}{1+exp\left(-\sum_{j=1}^{11} w_{1j}^H z_j + b_k^O\right)} \tag{9}$$

The combination of equations 8 and 9 leads to the mathematical formula for concentration of carbonyl taking into account all the inputs x_i:

$$[CO] = \frac{1}{1+exp\left(-\sum_{j=1}^{11} w_{1j}^H exp\left(-\sum_{i=1}^{7} w_{ji}^I x_i + b_j^H\right) + b_k^O\right)} \tag{10}$$

These mathematical formulas for calculating the carbonyl index and concentration of carbonyl contain just the required degree of complexity, and thus can readily be applied in polymeric industry as a contribution in the aim of enhancing the representativeness of accelerated aging testing methodologies and predicting the lifetime of polymers (PVC, PP, PS, PE, LDPE and EPDM) parts.

III.2. Comparison between ANN models

The two ANN models ANN1 and ANN2 were compared in terms of the mean absolute error

Table 4 shows a comparison between the NNs models. The performance of each model was evaluated in terms of the *MAE* and the *RMSE*. This clearly demonstrates that the ANN2 model developed in this work gave lower errors than ANN1 model. The results of the comparison are explained by the fact that ANN2 model takes into

(*MAE*) and the *RMSE*. *MAE* is distinct as follows [50-52]:

$$MAE = \frac{1}{n}\sum_{i=1}^{n}\left|(Y_{i,exp} - Y_{i,cal})\right| \qquad \textbf{(11)}$$

consideration the difference between additives and polymers, unlike the ANN1 model that does not differentiate between the two. Therefore, the ANN2 provides more accuracy than ANN1 model in estimating the carbonyl index and concentration of carbonyl in polymer materials.

Table 4. *Comparison between ANN1 and ANN2 models*

		ANN1	ANN2
MAE	**min**	4.8143e-06	8.8636e-05
	Mean	0.0623	0.0177
	Max	0.7066	0.2056
RMSE	**min**	4.8143e-06	8.8636e-05
	Mean	0.0958	0.0291
	Max	0.7066	0.2056

III.3. Sensitivity analysis

The contribution of the input variables on the outputs (carbonyl index and concentration of carbonyl) was determined by a sensitivity analysis using the "Weight" method for both neural network models (ANN1 and ANN2). This method, proposed initially by [53] and repeated by [54], provides a quantification of the relative importance (RI) of the inputs on the output of neural network [55]. It is based on the partitioning of connection weights between [16]: **(1)** the input-hidden layer, **(2)** the hidden-output layer. The contributions of the input variables obtained by the "weight" method for each ANN are listed in Figure 3 where it can be seen that all selected inputs influence the carbonyl index and concentration of carbonyl. The most influential inputs are: ρ_P=18.19% for ANN1 and X_3=21.06% for ANN2.
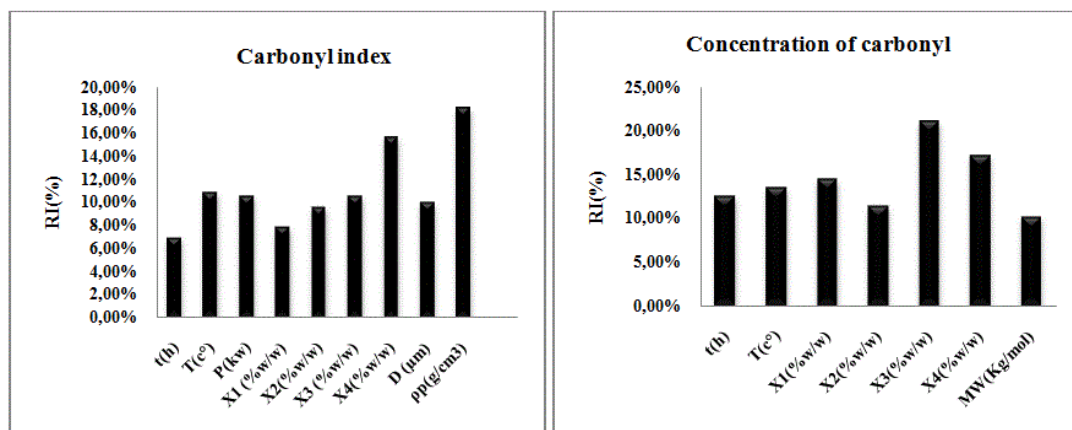
Figure 3. *Relative importance (RI) of input variables histograms: carbonyl index and concentration of carbonyl*

IV. Conclusion

In summary, artificial neural networks technique with a feed-forward back propagation algorithm was used to predict the carbonyl groups during photo-thermal and thermal aging of polymers. The purpose of the current study was the development of two feed-forward neural network models capable of predicting the carbonyl index and concentration of carbonyl in polymer materials. The ANN models developed in this work presented good performances (R=0.9471 for ANN1 and R=0.9830 for ANN2) with lower errors (*RMSE* equal to 0.0958 and 0.0291 for ANN1 and ANN2, respectively). The sensitivity analysis identified that all input variables have a major influence over the carbonyl index and concentration of carbonyl in polymers during photo-thermal and thermal aging. The most influential inputs are: ρ_P=18.19% for CI and X_3=21.06% for [CO]. The results of this work demonstrated that the ANN have a strong modeling capability and are able of solving problems in which the correlation between the inputs and the output is, not only nonlinear, but also much more complex. Last of all, ANN technique are confirmed to be a useful mathematical tool with a high potential for the prediction of the carbonyl index during the photo-thermal aging of polymers and the concentration of carbonyl during the thermal aging of polymers.

V. References

1. Ito, M.; Nagai, K. Degradation issues of polymer materials used in railway field. *Polym Degrad Stabil* 93 (2008) 1723-1735.
2. Robert, L.; Hastie, Jr.; Morris, D.H. The effects of physical aging on the creep response of a thermoplastic composite. *Virginia: American society for testing and materials International* 1 (1993) 163-186.
3. Hatada, K.; Fox, R.B.; Kahovec, J.; Marikhal, E.; Mita, I.; Shibaev, V. Definitions of terms relating to degradation, aging, and related chemical transformations of polymers. *IUPAC* 68 (1996) 2313-2323.
4. Shibryaeva, L. Thermal Oxidation of Polypropylene and Modified Polypropylene-Structure Effects. In Polypropylene. InTech (2012).
5. Strlič, M., Kolar, J. (Eds.). Ageing and stabilisation of paper. Ljubljana: National and university library (2005).
6. Yousif, E.; Haddad, R. Photodegradation and photostabilization of polymers, especially polystyrene: review. *Springerplus* 2 (2013) 398.
7. Colin, X.; Teyssedre, G.; Fois, M. Ageing and degradation of multiphase polymer systems. Handbook of Multiphase Polymer Systems (2011) 797-841.
8. Lacoste, J.; Therias, S. Vieillissement des matériaux polymères et des composites. *L'Act. Chim* (2015) 395.
9. Yousif, E.; Hameed, A.; Rasheed, R.; Mansoor, H.; Farina, Y.; Graisa, A.; Salih, N.; Salimon, J. Synthesis and photostability study of some modified poly(vinyl chloride) containing pendant benzothiazole and benzimidozole ring. *Int. J. Chem* 2 (2010) 65-80.
10. Yousif, E.; Hameed, A.; Salih, N.; Salimon, J.; Abdullah, B.M. New photostabilizers for polystyrene based on 2,3-dihydro-(5-mercapto-1,3,4-oxadiazol-2-yl)-phenyl-2-(substituted)-1,3,4-oxazepine-4,7-dione compounds. *Springerplus* 2 (2013) 104.
11. François-Heude, A.; Richaud, E.; Desnoux, E.; Colin, X. A general kinetic model for the photothermal oxidation of polypropylene. *J Photoch Photobio A* 296 (2015) 48-65.
12. Yousef, B.F.; Mourad, A.H.I.; Hilal-Alnaqbi, A. Prediction of the Mechanical Properties of PE/PP Blends Using Artificial Neural Networks. *Procedia Eng* 10 (2011) 2713-2718.
13. Koca, A.; Oztop, H.F.; Varol, Y.; Koca, G.O. Estimation of solar radiation using artificial neural networks with different input parameters for Mediterranean region of Anatolia in Turkey. *Expert Syst Appl* 38 (2011) 8756-8762.
14. Khaouane, L.; Benkortbi, O.; Hanini, S.; Si-Moussa, C. Modeling of an industrial process of pleuromutilin fermentation using feedforward neural networks. *Braz J Chem Eng*, 30 (2013) 105-116.
15. Hamadache, M.; Khaouane, L.; Benkortbi, O.; Si-Moussa, C.; Hanini, S.; Amrane, A. Prediction of Acute Herbicide Toxicity in Rats from Quantitative Structure–Activity Relationship Modeling. *Environ. Eng. Sci* 31 (2014) 243-252.
16. Ammi, Y.; Khaouane, L.; Hanini, S. Prediction of the rejection of organic compounds (neutral and ionic) by nanofiltration and reverse osmosis membranes using neural networks. *Korean J Chem Eng* 32 (2015) 2300-2310.
17. Rezrazi, A.; Hanini, S.; Laidi, M. An optimisation methodology of artificial neural network models for predicting solar radiation: a case study. *Theor Appl Climatol* 123 (2016) 769-783.
18. Khayet, M.; Cojocaru, C.; Essalhi, M. Artificial neural network modeling and response surface methodology of desalination by reverse osmosis. *J Membrane Sci* 368 (2011) 202-214.
19. Khajeh, M.; Kaykhaii, M.; Hashemi, S.H.; Shakeri, M. Particle swarm optimization-artificial neural network modeling and optimization of leachable zinc from flour samples by miniaturized homogenous liquid-liquid microextraction. *J Food Compos Anal* 33 (2014) 32-38.
20. Karakoç, M.B.; Demirboğa, R.; Türkmen, İ.; Can, İ. Effect of expanded perlite aggregate on cyclic thermal loading of HSC and artificial neural network modeling. *Sci. iran A* 19 (2012) 41-50.
21. Zhang, Z.; Friedrich, K. Artificial neural networks applied to polymer composites: a review. *Compos Sci Technol* 63 (2003) 2029-2044.
22. El Kadi, H. Modeling the mechanical behavior of fiber-reinforced polymeric composite materials using artificial neural networks—A review. *Compos. Struct* 73 (2006) 1-23.
23. Jiang, Z.; Zhang, Z.; Friedrich, K. Prediction on wear properties of polymer composites with artificial neural networks. *Compos Sci Technol* 67 (2007) 168-176.
24. Jiang, Z.; Gyurova, L.A.; Schlarb, A.K.; Friedrich, K.; Zhang, Z. Study on friction and wear behavior of polyphenylene sulfide composites reinforced by short carbon fibers and sub-micro TiO2 particles. *Compos Sci Technol* 68 (2008) 734-742.
25. Burgaz, E.; Yazici, M.; Kapusuz, M.; Alisir, S.H.; Ozcan, H. Prediction of thermal stability, crystallinity and thermomechanical properties of poly(ethylene oxide)/clay nanocomposites with artificial neural networks. *Thermochim. Acta* 575 (2014) 159-166.
26. Haykin, S. Neural Networks: A Comprehensive Foundation, Prentice Hall PTR. Upper Saddle River, NJ, USA (1998).
27. Silva, R.G.; Cruz, A.J.G.; Hokka, C.O.; Giordano, R.L.C.; Giordano, R.C.A hybrid feedforward neural network model for the cephalosporin C production process. *Braz J Chem Eng* 17 (2000) 587-598.
28. Si-Moussa, C.; Hanini, S.; Derriche, R.; Bouhedda, M.; Bouzidi, A. Prediction of high-pressure vapor liquid equilibrium of six binary systems, carbon dioxide with six esters, using an artificial neural network model. *Braz J Chem Eng* 25 (2008) 183-199.
29. Allen, N.S. Interaction between titanium dioxide pigments and hindered piperidine/antioxidant combinations in the photostabilisation of polypropylene. *Dyes Pigments* 3 (1982) 295-305.
30. Allen, N.S.; Khatami, H.; Thompson, F. Influence of titanium dioxide pigments on the thermal and photochemical oxidation of low density polyethylene film. *Eur Polym J* 28 (1992) 817-822.

31. Allen, N.S.; Edge, M.; Corrales, T.; Childs, A.; Liauw, C.; Catalina, F.; Peinado, C. Entrapment of stabilisers in silica: I.Controlled release of additives duringpolypropylene degradation. *Polym Degrad Stabil* 56 (1997) 125-139.
32. Peña, J.M.; Allen, N.S.; Edge, M.; Liauw, C.M.; Roberts, I.; Valange, B. Triplet quenching and antioxidant effect of several carbon black grades in the photodegradation of LDPE doped with benzophenone as a photosensitiser. *Polym Degrad Stabil* 70 (2000) 437-454.
33. Peña, J.M.; Allen, N.S.; Edge, M.; Liauw, C.M.; Valange, B. Studies of synergism between carbon black and stabilisers in LDPE photodegradation. *Polym Degrad Stabil* 72 (2001) 259-270.
34. Allen, N.S.; Edge, M.; Ortega, A.; Sandoval, G.; Liauw, C. M.; Verran, J.; Stratton, J.; McIntyre, R.B. Degradation and stabilisation of polymers and coatings: nano versus pigmentary titania particles. *Polym Degrad Stabil* 85 (2004) 927-946.
35. Yousif, E.; Salimon, J.; Salih, N. New photostabilizers for PVC based on some diorganotin (IV) complexes. *J Saudi Chem Soc* 19 (2015) 133-141.
36. Yousif, E.; Salimon, J.; Salih, N. New stabilizers for polystyrene based on 2-N-salicylidene-5-(substituted)-1,3,4-thiadiazole compounds. *J Saudi Chem Soc* 16 (2012) 299-306.
37. Yousif, E.; Salimon, J.; Salih, N.; Jawad, A.; Win, Y.F. New stabilizers for PVC based on some diorganotin(IV) complexes with benzamidoleucine. *Arab J Chem* 9 (2016) S1394-S1401.
38. Yousif, E.; Ahmed, A.; Abood, R.; Jaber, N.; Noaman, R.; Yusop, R. Poly(vinyl chloride) derivatives as stabilizers against photodegradation. *J Taibah Univ Sci* 9 (2015) 203-212.
39. Yousif, E. Triorganotin (IV) complexes photo-stabilizers for rigid PVC against photodegradation. *J Taibah Univ Sci* 7 (2013) 79-87.
40. Bannouf, W. Analyse et modélisation cinétique de la perte physique et de la consommation chimique d'un mélange phénol/HALS au cours du vieillissement radio-thermique d'une matrice EPDM (Thèse de doctorat. Ecole nationale supérieure d'arts et métiers-ENSAM) (2014).
41. Mkacher, I. Vieillissement thermique des gaines PE et PVC de câbles électriques (Thèse de doctorat. Arts et Métiers ParisTech) (2012).
42. Yousif, E.; Yusop, R.M.; Ahmed, A.; Salimon, J.; Salih, N. photostabilizing efficiency of PVC based on epoxidized oleic acid. *MJAS* 19 (2015) 213-221.
43. Yousif, E.; Salimon, J.; Salih, N. Improvement of the photostabilization of PVC films in the presence of thioacetic acid benzothiazole complexes. *MJAS* 15 (2011) 81-92.
44. Pons, C. Durabilité des géomembranes en polyéthylène haute densité utilisées dans les installations de stockage de déchets non dangereux (Thèse de doctorat. Paris Est) (2012).
45. Xia, L.; Wu, H.; Guo, S.; Sun, X.; Liang, W. Enhanced sound insulation and mechanical properties of LDPE/mica composites through multilayered distribution and orientation of the mica. *Compos Pt A Appl Sci Manuf* 81 (2016) 225-233.
46. Mnif, N. Elaboration et caractérisation de mélanges complexes à base de polypropylène en vue de son écoconception et de son recyclage dans les véhicules hors d'usage (Thèse de doctorat. Lyon, INSA) (2008).
47. Chebil, M.S. Etude de films ultraminces de polystyrène par réflectivité des rayons X et ellipsométrie en fonction de leur exposition à du CO2 (Thèse de doctorat. Le Mans) (2013).
48. Laidi, M.; Hanini, S. Optimal solar COP prediction of a solar-assisted adsorption refrigeration system working with activated carbon/methanol as working pairs using direct and inverse artificial neuralnetwork. *Int J Refrig* 36 (2013) 247-257.
49. Hamadache, M.; Benkortbi, O.; Hanini, S.; Amrane, A.; Khaouane, L.; Si-Moussa, C. A Quantitative Structure Activity Relationship for acute oral toxicity of pesticides on rats: Validation, domain of application and prediction. *J Hazard Mater* 303 (2016) 28-40.
50. Hamadache, M.; Hanini, S.; Benkortbi, O.; Amrane, A.; Khaouane, L.; Si-Moussa, C. Artificial neural network-based equation to predict the toxicity of herbicides on rats. *Chemom Intell Lab Syst* 154 (2016) 7-15.
51. Khaouane, L.; Ammi, Y.; Hanini, S. Modeling the Retention of Organic Compounds by Nanofiltration and Reverse Osmosis Membranes Using Bootstrap Aggregated Neural Networks. *Arab J Sci Eng*, 42 (2017) 1443-1453.
52. Maouz, H.; Khaouane, L.; Hanini, S.; Ammi, Y. Modeling the molecular weight and number average molecular masses during the photo-thermal oxidation of polypropylene using neural networks. *Moroccan Journal of Chemistry*, 7 (2019) 017-027.
53. Garson, G.D. Interpreting neural network connection weights. *Artif Intell Expert* 6 (1991) 46-51.
54. Goh, A.T. Back-propagation neural networks for modeling complex systems. *Eng Appl Artif Intel* 9 (1995) 143-151.
55. Gevrey, M.; Dimopoulos, I.; Lek, S. Review and comparison of methods to study the contribution of variables in artificial neural network models. *Ecol Model* 160 (2003) 249-264.

Please cite this Article as:

Maouz H., Khaouane L., Hanini S., Ammi Y., Laidi M., Benimam H., The prediction of carbonyl groups during photo-thermal and thermal aging of polymers using artificial neural networks, ***Algerian J. Env. Sc. Technology, 6:3 (2020) 1448-1456***